

LASER INTERFEROMETER GRAVITATIONAL WAVE OBSERVATORY
- LIGO -
CALIFORNIA INSTITUTE OF TECHNOLOGY
MASSACHUSETTS INSTITUTE OF TECHNOLOGY

Technical Note	LIGO-T2200160-v1	2022/09/22
Higher Order Mode Coupling Analysis and Thick Lens Modeling		
Peter Carney, Rana X. Adhikari, Shruti Jose Maliakal		

California Institute of Technology
LIGO Project, MS 18-34
Pasadena, CA 91125
Phone (626) 395-2129
Fax (626) 304-9834
E-mail: info@ligo.caltech.edu

Massachusetts Institute of Technology
LIGO Project, Room NW22-295
Cambridge, MA 02139
Phone (617) 253-4824
Fax (617) 253-7014
E-mail: info@ligo.mit.edu

LIGO Hanford Observatory
Route 10, Mile Marker 2
Richland, WA 99352
Phone (509) 372-8106
Fax (509) 372-8137
E-mail: info@ligo.caltech.edu

LIGO Livingston Observatory
19100 LIGO Lane
Livingston, LA 70754
Phone (225) 686-3100
Fax (225) 686-7189
E-mail: info@ligo.caltech.edu

Contents

1	Introduction	3
I	Thick Lens Model	4
2	PSOMA Tabletop Set Up and Simplifications	4
3	ABCD Matrix	5
4	Thin and Thick Lens Comparison	6
5	Next Steps for Thick Lens Analysis	6
II	Higher Order Mode Coupling Model	8
6	Lens Aberrations	8
7	Higher Order Mode Coupling	9
8	Using Python and Mathematica	12
9	Distribution of Coupling Coefficients	13
10	Analyzing Mode Mismatch	16
11	Future Steps	18
	11.1 Using Different functions for $Z(R, x, y)$	18
	11.2 Using Two Lenses	19

Abstract

Though only at the tabletop stage, future gravitational wave detectors aim to include a Phase Sensitive Optomechanical Amplifier (PSOMA) to help mitigate LIGO readout losses. The triangular cavity of the PSOMA is experiencing mode mismatch, which leads us to examine our mode matching lenses. The original method of analysis was to model the tabletop configuration while taking lens thickness into account. This became straightforward to model for a given set of mode matching lenses, yet the research took a more general and fundamental direction in analyzing lens aberrations for Gaussian beams. A conceptual idea of the cause and effects of lens aberrations, inspired the use of a modal coupling method to quantify mode mismatch. This method details how Gaussian beams propagating through curved optics can couple into higher order modes. Though still in the beginning stages, the research provides valuable results on how not only the PSOMA lenses, but LIGO optics in general contribute to higher order mode noise.

1 Introduction

The majority of this paper discusses a general property of Gaussian beams and analyzes the modal coupling from the fundamental Gaussian mode into higher order modes upon propagation through a given surface. However, the impetus for the topic came from the mode mismatch of a tabletop design of a Phase Sensitive Optomechanical Amplifier (PSOMA), which aims to be implemented in next generation LIGO [1].

Currently, the PSOMA uses two convex - planar lenses to assist in mode matching the laser into a three mirror ring cavity. With proper alignment and positioning, the cavity still finds itself mode mismatched. There are two main directions taken to analyze the mode mismatch.

First, lens thickness is taken in account in modeling of the tabletop setup. Originally, a thin lens approximation was used in aiding the configuration of the design. To model a thick lens, the ABCD matrix approach becomes useful. It gives direct numeric results which are easily comparable to a thin lens model. Further analysis of these results may lead to more accuracy in configuring LIGO optics for higher mode matching and resonances.

The second direction is a modal coupling analysis [10]. This approach originates from the study of lens aberrations - in particular spherical aberrations. The cause and characterizations of spherical aberrations are largely understood with light rays, yet implementing them with Gaussian beams for mode mismatch is not trivial. A fundamental understanding of how aberrations work give a backbone to using a modal coupling method. This is where the research takes a much more general direction. Upon propagation through a single curved surface, scattering from the pure Gaussian mode into higher order Hermite and Laguerre Gauss modes becomes modeled to quantify mode mismatch. In practice, multiple lenses are used to minimize this effect, yet for the purposes of this project, the propagation through only one curved surface (which can be thought of as a convex lens surface) will be analyzed. Results from this approach give insight on the conditions in which higher order modes arise. Much more research can be done than what is currently given in this paper. Upon further exploration of the modal coupling approach, higher order modes and mode mismatch within optical cavities can be significantly decreased in not just the PSOMA design, but in LIGO.

This paper will start by addressing how a thick lens is modeled and explain which parameters are used to compare between thick and thin lens analyses. It will then discuss the next steps of utilizing the results of thick lens model. In the second part, the paper will move into the modal coupling analysis. A background on the modal coupling method will be addressed, followed by detailing how the numerical and analytical modeling were done in python and Mathematica respectively. The paper will discuss results of the modal coupling approach, and then detail next research steps.

Part I

Thick Lens Model

2 PSOMA Tabletop Set Up and Simplifications

In order to truly show the analytical ABCD matrix model, a visual of the set up, and simplification must be shown first. The configuration of the three mirror PSOMA cavity is shown in Figure 1(a). The beam is focused using two lenses, and aligned using two steering mirrors. The beam waist within the cavity is between MC2 and MC3.

This configuration is taken and simplified in order to perform the ABCD matrix evaluation [11]. The beam waist position between MC2 and MC3 is taken to be half of its propagation distance within the cavity. This distance becomes the length of the simplified cavity of Figure 1(b), meaning that the beam waist in the simplification diagram is at MC2. SM1 and SM2 are neglected, as they are both planar mirrors and don't contribute to the transformation of the q parameter in the ABCD calculation. The only components considered are lengths L_1 , L_2 , and L_3 , and focal lengths f_1 and f_2 , which become used in the thin lens ABCD calculation.

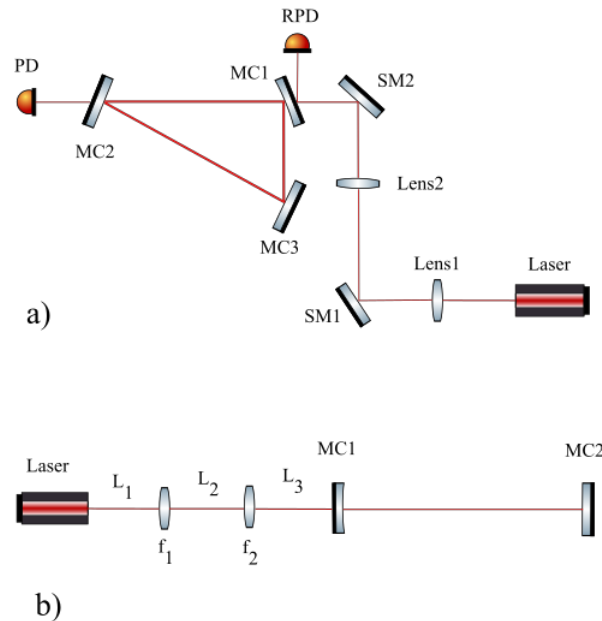


Figure 1: a) Diagram of current ring cavity configuration. Note that MC1 has a ROC of 2m, while MC2 and MC3 are both flat mirrors. The beam waist within the cavity is between MC2 and MC3. b) Simplification from a ring cavity to Fabry-Perot cavity. f_1 and f_2 denote focal lengths of each lens.

3 ABCD Matrix

Each optical component (including free space) is represented with a 2x2 square matrix that acts upon the q parameter of the Gaussian beam and transforms it. As a beam propagates through multiple optical components, each matrix becomes multiplied together, and the four indices of the resulting matrix act as components A, B, C and D. These matrix components act on the beam's initial q parameter, q_1 , and transform it to q_2 . [5]

A thin lens is denoted with matrix:

$$\begin{pmatrix} 1 & 0 \\ \frac{-1}{f} & 1 \end{pmatrix}$$

An ABCD matrix calculation that transforms the beam from the laser source to the first mirror of the Fabry-Perot cavity model of Figure 1(b) will be:

$$\begin{pmatrix} 1 & L_3 \\ 0 & 1 \end{pmatrix} \begin{pmatrix} 1 & 0 \\ \frac{-1}{f_2} & 1 \end{pmatrix} \begin{pmatrix} 1 & L_2 \\ 0 & 1 \end{pmatrix} \begin{pmatrix} 1 & 0 \\ \frac{-1}{f_1} & 1 \end{pmatrix} \begin{pmatrix} 1 & L_1 \\ 0 & 1 \end{pmatrix} = \begin{pmatrix} A & B \\ C & D \end{pmatrix}$$

Which gives the q_2 parameter in the equation [5] [7]:

$$\frac{q_2}{n} = \frac{A \frac{q_1}{n} + B}{C \frac{q_1}{n} + D} \quad (1)$$

In which n is the index of refraction of the medium through which the beam propagates. For the tabletop cavity, this is air.

Considering that beam width is the direct parameter of the Gaussian beam that correlates to mode matching, q_2 can be decomposed to find the beam width:

$$\omega(z) = \sqrt{\frac{\lambda |q|^2}{\pi \Im(q)}} \quad (2)$$

In which $\omega(z)$ is the beam width, λ is the wavelength of the beam, and $\Im(q)$ is the imaginary portion of the q parameter.

When modeling for thick lenses, the distance within the lens along with the front and back radius of curvatures are all taken into account [9]. As a result, the matrix for a single thick lens becomes:

$$\begin{pmatrix} 1 & 0 \\ \frac{n'-n}{R_2} & 1 \end{pmatrix} \begin{pmatrix} 1 & d \\ 0 & 1 \end{pmatrix} \begin{pmatrix} 1 & 0 \\ \frac{n-n'}{R_1} & 1 \end{pmatrix}$$

In which R_1 and R_2 are the front and back side radius of curvatures, d is the index of refraction of the glass, and n' is the index of refraction of the glass. Multiplying all matrices of the two lens system generates a complex matrix, which can be run in an online matrix

calculator to obtain a set of A, B, C, and D components. Each component of the resulting matrix will be in the form of equations composed of optical parameters (such as R_1 , R_2 , L_1 ... etc). These equations can be evaluated in Python or Matlab to find the width $\omega(z)$ at specific points in the propagation.

4 Thin and Thick Lens Comparison

	$\omega(z)$ before MC1	$\omega(z)$ at MC2
Thin Lens	0.5443mm	0.3702mm
Thick Lens	0.5475mm	0.3763mm

Table 1: Comparative beam widths of the simplified triangular cavity.

The ABCD calculation for thin and thick lenses were numerically evaluated in python. They are currently written so that the parameters of design can be defined independently, and then evaluated to give the width $\omega(z)$ of the beam in two separate places: upon entering the first mirror of the cavity, MC1, and at the beam waist within the cavity (which is MC2 in this simplification). There is a change on the order of micrometers when considering lens thickness.

A quantitative result of the fractional mode matching power can be obtained from these measurements. The formula to find this would be:

$$Mode\ Matching = 1 - \left(\frac{|\omega_{thick} - \omega_{thin}|}{\omega_{thick}} \right)^2 \quad (3)$$

Where ω_{thick} is the beam width using thick lens approach, and ω_{thin} is the beam width using thin lens approach. The left hand side of the equation will be a fraction of the mode matching power, which is a number between 0 to 1 where 1 represents being 100% mode matched. With the PSOMA tabletop parameters and results of the thin and thick lens analyses, the mode matching percentages are 99.99658% before MC1, and 99.9737% at MC2.

5 Next Steps for Thick Lens Analysis

Considering this is a simplification of a three mirror cavity, a useful approach would be to fully model a triangular cavity using software package FINESSE [3]. By adding a detector for the power transmitted in FINESSE (which would be located at the PD of Figure 1(a)), resonance conditions can be found. One can model a scenario in which the positions of the two mode matching lenses are tuned to give maximum power transmitted. Tuning the positions of the lenses changes in the beam width at many points of its propagation. If one then writes a component in FINESSE measuring the width of the beam as it enters the first mirror of the cavity, then the power transmitted can be used to determine which beam width entering the cavity at MC1 will create maximum resonance. In other words, FINESSE can

be used to find the cavity eigenmode width.

FINESSE is assumed to use a thin lens approximation in its compiling, so it becomes necessary to implement the thick lens ABCD matrix numerical model. The reason the thin lens ABCD numerical model will not be used to find the ideal cavity beam width is because it simplifies the model from a three mirror cavity into a Fabry-Perot cavity, thus losing its anti-symmetric aspects. Using FINESSE can generate an accurate beam width for three mirror anti-symmetric cavity resonance.

Once the ideal beam width for resonance is found, one can then use the thick lens evaluation in python to generate a 2D tolerance map (or heat/contour plot) to that specific beam width. Ideally, it should be a tolerance for how the beam width (at a given position such as right before MC1) deviates from its eigenmode value as a function of lens 1 and lens 2 position. This can be used to precisely find the ideal positions of the two mode matching lenses, and then implemented in the tabletop set up to determine how much using thick lens model affects the mode matching.

Part II

Higher Order Mode Coupling Model

6 Lens Aberrations

This section provides a basic introduction to the principles behind lens aberrations, which inspires the use of a modal coupling approach in this research.

Spherical aberrations arise from the light at the edges of a spherical surface refracting more than light near the center, [2] [12] resulting in multiple focal points for varying rays, as seen in Figure 1(a), points C, B, A, and F along the propagation axis. This results in a blurred image.

Ray tracing illustrates that the further away from the center of the lens the light prop-

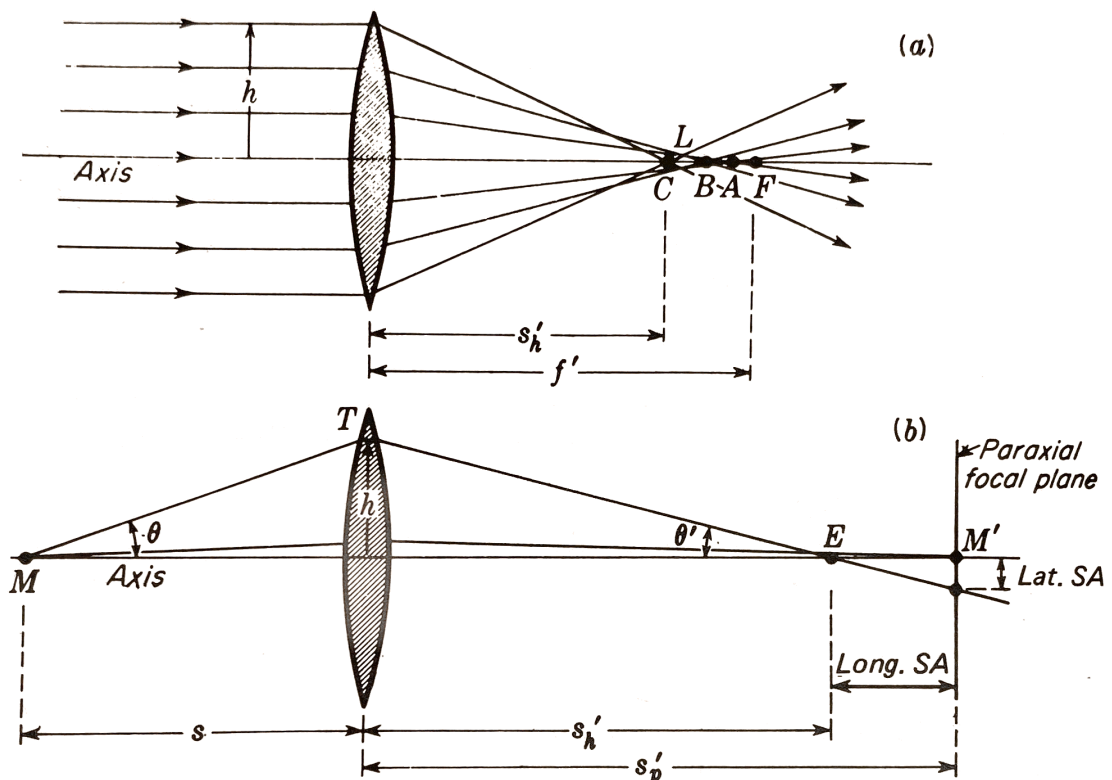


Figure 2: From *Fundamentals of Optics* Francis A. Jenkins and Harvey E. White. Chp. 9 (a) Diagram of how lens aberrations occur, and how they can be perceived. (b) Notice here the Longitudinal Spherical Aberrations (Long. SA) and Latitudinal Spherical Aberrations (Lat. SA).

gates, the larger the distance between its focusing point, s'_h , and the paraxial focal point f' . This difference can be quantified using ray tracing geometry and algebra. Under ideal circumstances, the distance of the focal point can be found with a first order approximation of sine, since the angle θ shown in Fig 2(b) is small. However, spherical aberrations can be quantified if a third order sine approximation is used [4].

$$\sin(\theta) \approx \theta - \frac{\theta^3}{3!} \quad (4)$$

When using a third order to solve for the image length, the equation used to quantify lens aberrations for rays of light becomes [4]:

$$\frac{n}{s} + \frac{n'}{s'_h} = \frac{n' - n}{r} + \left[\frac{h^2 n^2 r}{2 f' n'} \left(\frac{1}{s} + \frac{1}{r} \right)^2 \left(\frac{1}{r} + \frac{n' - n}{n s} \right) \right] \quad (5)$$

In which the left side of the equation depicts the magnitude of the aberration, and the right is dependent on a multitude of factors. The aberration size is directly proportional to h^2 . This is consistent with Figure 1(a), and the original characterizations for lens aberration behavior.

Considering this phenomena, it must be considered for Gaussian beams, however, going directly from ray tracing to Gaussian beams is not trivial. At the moment, there is no quantified correlation of how varying focal points of light equate to the creation higher order modes, or mode mismatch in an optical cavity. Thus, a modal coupling approach is used for Gaussian beams. The basic principle that aberrations arise from a large width of light focusing in a spherically curved lens inspires the analysis to be done using modal coupling.

Spherical aberrations can heavily be mitigated with the use of multiple lenses to refocus the light, or with specially curved optics so that the light will all refract to the same location [2]. These principles will also be taken into account when using the modal coupling method, and dicussed for further research.

7 Higher Order Mode Coupling

The modal coupling approach heavily relies on Gaussian beam modeling. Starting from the general form of a Gaussian beam:

$$E(x, y, z) = E_0 e^{-i(\omega t - kz)} \frac{\omega_0}{\omega(z)} e^{\left(-ik \frac{x^2 + y^2}{2R(z)} - \frac{x^2 + y^2}{\omega(z)} \right)} e^{i\psi(z)} \quad (6)$$

Where k is the wave number, z is the position on the propagation axis, $R(z)$ is the Gaussian beam radius of curvature at z , ω_0 is the beam waist, $\omega(z)$ is the beam width at z , and ψ is the Gouy phase. u is defined as:

$$u(x, y, z) = \sqrt{\frac{2}{\pi}} \frac{1}{\omega(z)} e^{\left(-ik \frac{x^2 + y^2}{2R(z)} - \frac{x^2 + y^2}{\omega(z)} \right)} e^{i\psi(z)} \quad (7)$$

Which represents the spatial properties of the beam, and is a solution to the paraxial wave approximation.

It is generally known that upon misalignments, or unmatched curve fronts between the beam and the optic, families of higher order modes can arise. The two families of focus will be the Hermite-Gauss (HG) modes, and Laguerre-Gauss (LG) modes. These families of modes are each described as a set equations of $u(x, y, z)$ that are solutions to the paraxial wave equation. The HG modes for a Gaussian beam have the form:

$$u_{nm}(x, y, z) = (2^{n+m-1}n!m!\pi)^{-1} \frac{1}{\omega(z)} e^{i(n+m+1)\psi(z)} H_n \frac{\sqrt{2}x}{\omega(z)} H_m \frac{\sqrt{2}y}{\omega(z)} e^{\left(-ik \frac{x^2+y^2}{2R(z)} - \frac{x^2+y^2}{\omega(z)}\right)} \quad (8)$$

While the LG modes have the form:

$$u_{pl}(r, \phi, z) = \frac{1}{\omega(z)} \sqrt{\frac{2p!}{\pi(|l|+p)!}} e^{i(2p+|l|+1)\psi(z)} \left(\frac{\sqrt{2}r}{\omega(z)}\right)^{|l|} L_p^{|l|} \left(\frac{2r^2}{\omega(z)^2}\right) e^{(-ik \frac{r^2}{2q(z)} + il\phi)} \quad (9)$$

The set of polynomials H_n and H_m correspond to HG modes and $L_p^{|l|}$ correspond to LG. The indices, n, m and p, l are whole integers that denote the order of the mode. In both families, each and every mode is a solution to the paraxial wave equation, meaning they represent an infinite set of orthonormal basis vectors. As a result, the inner product yields:

$$\iint_{-\infty}^{\infty} u_{nm} u_{n'm'}^* dx dy = \delta_{nn'} \delta_{mm'} \quad (10)$$

The same is applicable to u_{pl} . Given this property, it is possible to construct an inner product that produces a coupling coefficient, used to represent the scattering from the pure Gaussian, 0 0 mode to any higher order mode. Considering just Hermite in the following:

$$c_{nmn'm'} = \iint_{-\infty}^{\infty} u_{nm} u_{n'm'}^* e^{(2ikZ(x,y))} dx dy \quad (11)$$

The $Z(x, y)$ is significant. It is a surface function representing an optical element with curvature in the propagation path of the Gaussian beam. With any given curved surface, the orthonormality becomes distorted, and components of the pure Gaussian mode (0, 0) couple into higher order modes. Given that the original inner product without the $Z(x, y)$ function produces 0 or 1, the magnitude of the coupling coefficient $|c_{nmn'm'}|$ will always be between 0 or 1. The amount that is coupled from the 0, 0 into higher order modes is represented by the $|c_{nmn'm'}|^2$.

From here on, since the coupling from only a pure Gaussian mode is considered, the coupling coefficients will be denoted c_{nm} (or c_{pl} for LG) in which $n, m = 0, 1, 2, 3...etc$.

It is assumed that $n', m' = 0$, which represents the pure Gaussian mode, and will be omitted from future syntax.

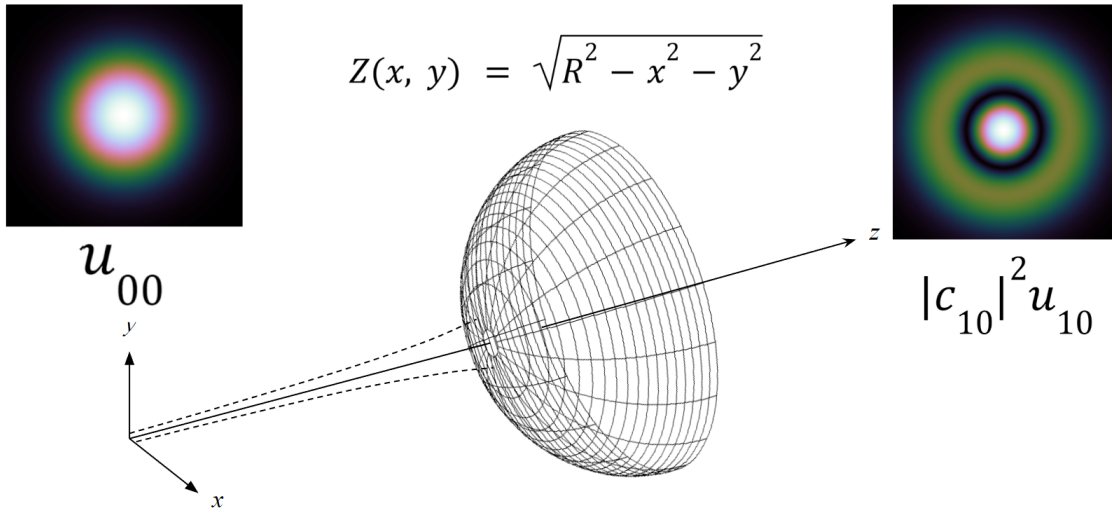


Figure 3: A visual of the process of the modal coupling propagation. Even though in the visual, $Z(R, x, y)$ is for a sphere facing opposite what is shown, when evaluated in the integration, it makes no difference in the outcome since it is in an imaginary part in which the absolute value is taken.

A visual of this process is illustrated in Figure 3. The semisphere represents an optical surface such as a lens or mirror. The beam propagates through the optic in the z direction. One specific coupling from the pure Gaussian mode on the left to the first LG higher order mode on the right is illustrated in the intensity patterns of the beam. The coefficient, $|c_{10}|^2$ represents the fraction of the initial power of the incoming Gaussian beam is coupled into that specific higher order mode.

After a beam propagates through a curved surface, it becomes a summation of the pure Gaussian mode and all higher order modes. Each spatial mode equation is multiplied by a fraction of how much power is coupled into that mode:

$$u(x, y, z) = \sum_{n,m=0}^{\infty} c_{nm} u_{nm}(x, y, z) \quad (12)$$

The resulting spatial field equation is then analyzed for its mode composition, width, and q parameter.

Much more detailed information on the mathematics of Gaussian beams can be found in *Interferometer Techniques for Gravitational-Wave Detection*, Chapter 9. [5]

8 Using Python and Mathematica

Both Python and Mathematica [13] were used in the process of constructing the Gaussian equations, and evaluating the inner product. In both programs, a spatial equation $u_{nm}(x, y, z)$ was written. Then, a complex conjugate, $u_{nm}^*(x, y, z)$ was written and multiplied to the original spatial equation, along with $e^{(2ikZ(x,y))}$.

It is key to note that the $Z(R, x, y)$ function has the form of a sphere as shown in Figure 3. R is the radius of curvature of the optic the beam propagates through.

Python evaluates its integral numerically by importing Scipy's `dqquad` function. This means that the Gaussian beam parameters (Rayleigh range, beam waist, beamfront radius of curvature, position z , etc) must be defined prior to numerical integration. This also means that the bounds of the integral cannot go to infinity, since Python takes a finite amount of steps to complete its integration. Thus, the integration bounds are manually set to encompass virtually all of the beam, and becomes:

$$\iint_{-1}^1 u_{nm} u_{n'm'}^* e^{(2ikZ(x,y))} dx dy$$

Depending on the size of the bounds, the Python `dblquad` function can run faster or slower, yet the integration will always generate a numerical answer. It is also important to note that the bounds are always well within the radius of curvature, so that Python will not evaluate a complex integral in which $x^2, y^2 > R^2$. Since c_{nm} itself a complex number however, it is necessary to explicitly keep the imaginary part of the integral in Python.

Mathematica is much more efficient in analytically evaluating the model. The integration is done to infinity here. However, the integration cannot be done unless a Taylor expansion is made to the function $Z(R, x, y)$. This is necessary since evaluating an x and y beyond a given radius of curvature R produces an error in the program. Therefore, in Mathematica, the equation becomes:

$$Z(R, x, y) = R \left(1 - \frac{(x^2 + y^2)}{2R^2} \right) \quad (13)$$

The program as of right now only runs integration for the second order expansion. Any higher order approximations evaluate to error functions.

The advantage of using Mathematica is that the beam parameters do not need to be previously defined. Once the integration is completed, Mathematica can generate an equation representing each coupling coefficient as a function of parameters such as optic radius of curvature, beam width, and wavenumber. For instance, the equation for the coupling of a pure Gaussian to another pure Gaussian in the Hermite basis is:

$$c_{00} = \frac{2e^{(2ikR)} R}{2R + ik\omega^2} \quad (14)$$

In which again, R is the radius of curvature of the $Z(R, x, y)$ function representing an optic, k is the wavenumber, and ω is the beam width.

These equations can then be taken and plotted in Mathematica to efficiently vary different parameters such as beam width or optic radius of curvature to better characterize how the higher mode coupling behaves.

Currently, Mathematica does not evaluate the integration Laguerre Gauss equations. It is suspected that the debugging must be done in the bounds of the integration. In its current set up, all of the steps leading up to the evaluation of the inner product are done the same format as the Hermite Gauss, with only a difference in coordinate systems, and using Laguerre Polynomials. However, Python can generate similar plots for the Laguerre basis that Mathematica does for the Hermite. These will be discussed in the next section.

9 Distribution of Coupling Coefficients

It has been discussed that for a Gaussian beam propagating through an optical surface, lens aberrations can be seen as the pure Gaussian mode coupling into higher order modes. A modal coupling simulation run in python has been evaluated with the parameters shown in Table 2.

It becomes relevant to determine how much power is distributed into higher order modes upon coupling. The relative power can be found by taking the square of the absolute value of the coupling coefficient. Considering that all functions are normalized, these values represent a fraction of the total power. In an ideal case, there should be no power scattered into higher order modes, and the beam should stay 100% in the pure Gaussian mode. However, the properties of lens aberrations are such that for light hitting a spherically curved surface, the light farther from the center will refract more, thus creating spherical aberrations. Equivalently, for Gaussian beams with larger beam width $\omega(z)$ relative to the optic they propagate through, there will be more power coupled into the higher order modes.

Wavelength	λ	1550 nm
Beam waist	ω_0	0.3482 mm
Position	z	61.7 mm
Beam width	$\omega(z)$	0.359 mm
Beamfront Radius of Curvature	Rc	1040.437 mm
Rayleigh Range	z_R	245.74 mm
Wavenumber	k	4053.67 m^{-1}
Gouy Phase	$\psi(z)$	0.2459

Table 2: Parameter specifications needed to complete numerical integration in python.

Note that all parameters can be derived from λ , ω_0 , and z . Derivations for these parameters can be found in: [5]

Considering the properties of aberrations, the research first examines how power is distributed through higher order modes for a given radius of curvature. Figure 4 illustrates this for a radius of curvature of 500mm. Approximately 78.55% is retained within the pure Gaussian mode in both HG and LG. For HG, only the even modes are shown. This is because in the inner product, any odd numbered index in a HG mode (such as $n \& m = 01, 10, 11, 12, 21, 23, 32...$ etc) creates a situation in which an odd function is integrated, making the inner product zero. The Hermite polynomials H_n and H_m referenced in equation 7 create the odd function whenever an odd index for n and m is chosen. Since the LG modes use a different coordinate system with different polynomials, this concept does not apply.

At first glance, it may appear that the LG has more power coupled into its higher order modes. However, since the n index represents a higher order mode in the x direction of propagation, and m is represented in the y direction, as a Gaussian beam undergoes a radially symmetric mode coupling, the next higher order mode can be thought of as a $c_{02} + c_{20}$. This combination is equivalent to the c_{10} LG higher order mode, carries a whopping 16.4% of the power. For Hermite, c_{02} and c_{20} each have 8.2% of the power, which together are equivalent to the c_{10} LG higher order mode.

A point to consider is how the distribution of higher order mode power varies as optic radius of curvature changes, and with beam width. As the radius of curvature increases, the beam becomes more focused towards the center of the optic, and visa versa. As shown in Figure 5, for optics with large radii of curvature compared to their incoming beam, little aberration is found, and most of the power resides in the pure Gaussian beam. However, as the radius of curvature decreases, more power is scattered into higher order modes.

Conversely, if the beam width is varied, this directly affects how close to the center the beam is focused. Figure 6 illustrates this effect, as smaller beams propagate with less mode coupling. Note that this graph was generated in Mathematica, in which the equation for c_{00} (Discussed in section 8) is used to vary $\omega(z)$.

At the moment, LG is not able to evaluate in Mathematica. Mathematica can only evaluate

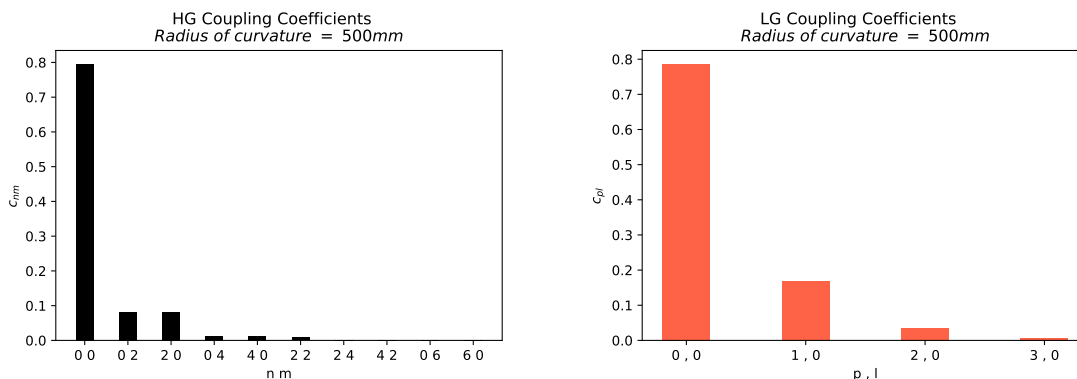


Figure 4: The distribution of coupling coefficients for propagation through a surface with radius of curvature = 500mm. This was evaluated in Python for a perfect spherical equation.

second order Taylor approximations (Discussed in section 8), which cannot be called a perfect sphere. However, this research has shown that there is virtually no difference between a $Z(x, y)$ function with a second order Taylor approximation and a function modeled as a perfect sphere. This will be discussed further in section 11.

Using this information, after a Gaussian beam has propagated through a surface, a tolerance can be constructed to find conditions in which the beam will stay Gaussian, and not scatter. Less higher order mode coupling occurs when the ratio of beam size to optic size is smaller.

To illustrate this, the fraction of power in the pure Gaussian mode, $|c_{00}|^2$, can be taken and plotted against both radius of curvature and beam width, which is shown in Figure 7. The relationship between the ratio of beam width to optic size and the fraction of residual power in the pure Gauss mode is outlined in this figure. This can ideally be used to find an optimal

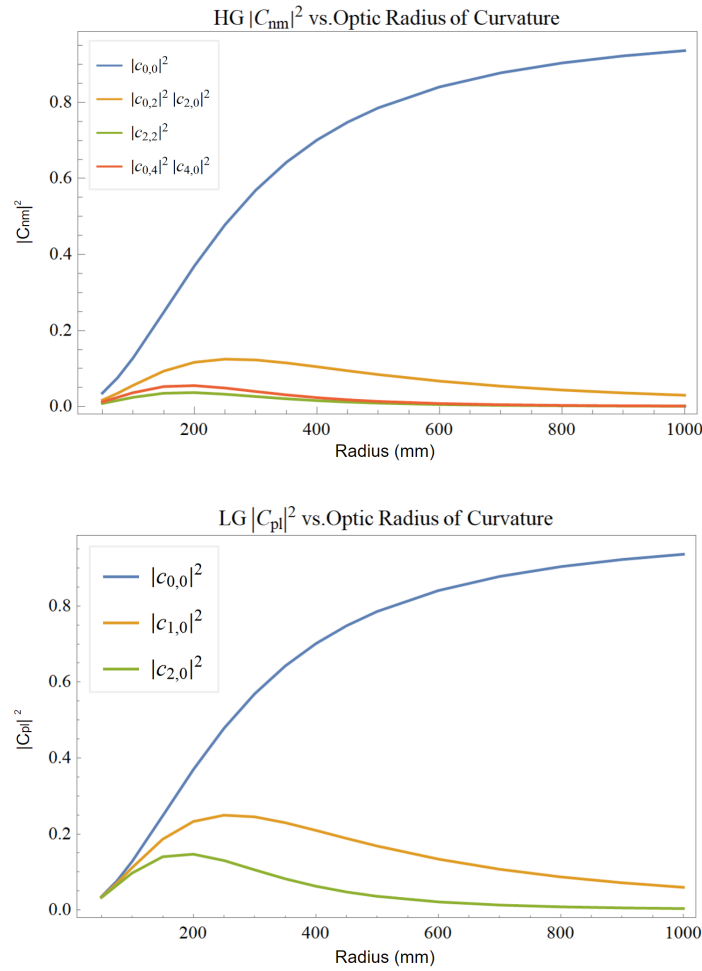


Figure 5: The HG and LG Coupling coefficients as a function of R , the radius of curvature of the optical surface. In both cases, the blue curves representing c_{00} are the pure Gaussian mode of the beam. This was evaluated in Python for a perfect spherical equation.

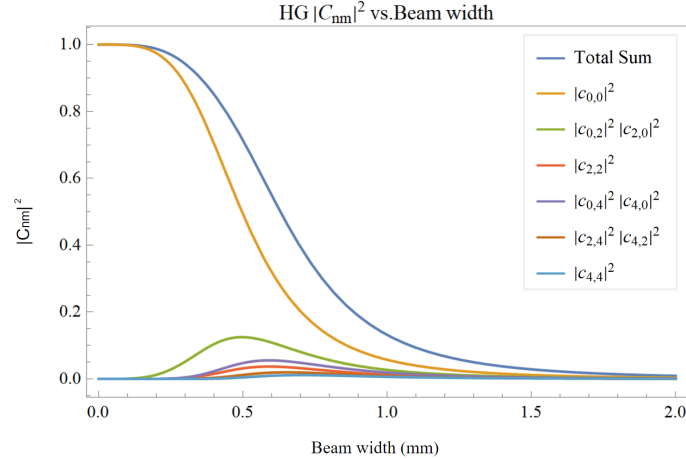


Figure 6: The HG coupling coefficients as a function of incoming beam width. The Radius is fixed at 500mm. The blue curve illustrates the summation of all the curves.

configuration of beam width to lens curvature.

10 Analyzing Mode Mismatch

Quantifying mode mismatch is not a trivial task. It can be expressed as [10]:

$$MM = 1 - |c_{00}|^2 \quad (15)$$

In which MM is a measure of mode mismatch. Naturally, as $MM \rightarrow 0$, the more purely Gaussian the beam is. As $MM \rightarrow 1$, the more coupling there is into higher order modes.

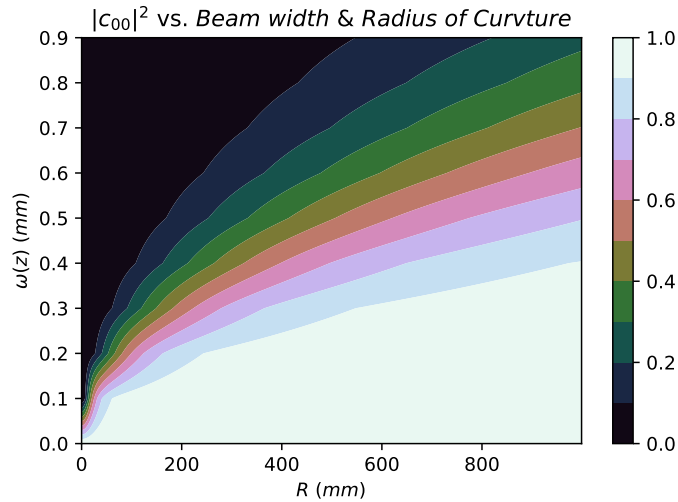


Figure 7: The fractional power in the Gaussian mode after propagation through a lens. This contour plot is generated by varying Radius of curvature and beam width

Mode mismatch can be plotted in the same fashion as the fractional power in the previous section. Figure 8 shows this. Again, the same trend shows that larger radii of curvature relative to a given beam waist correspond to better mode match.

The original endeavor of this paper was to more accurately evaluate the mode mismatch as it relates to an optical cavity, and finding the beam width with this model is more effective. As mentioned in section 8, the beam after propagation through a curved surface is a superposition of all higher order modes with their respective power distributions. The resulting intensity pattern can be used to find the width of the beam, and then compared to the ABCD matrix approach.

Using the same configurations as the previous section, an intensity pattern can be generated in Python. Since the fractional power distribution for this configuration is already known, a superposition of higher order mode intensity patterns can be plotted. In Figure 8, the intensity patterns are normalized. The higher order mode superposition is slightly distorted compared to the pure Gaussian distribution.

This visualization can give an idea of how the beam width should be affected upon propagation through a surface that induces higher order mode coupling. The width, $\omega(z)$ is defined by the position in which the intensity is $\frac{1}{e^2}$ of its maximum value [5]. Evaluating this position can be done in Python. For the given configuration shown in section 10, the beam width is shown in table 10, along with the width found from the ABCD matrix approach for the same configuration. The beam width is distorted by $\approx 2\mu m$.

Modal Coupling	0.35667 mm
ABCD Matrix	0.3590 mm

Table 3: Comparison of beam width after propagation through an optic with a radius of curvature of 500mm. For modal coupling approach, this curvature, again, refers to the R in

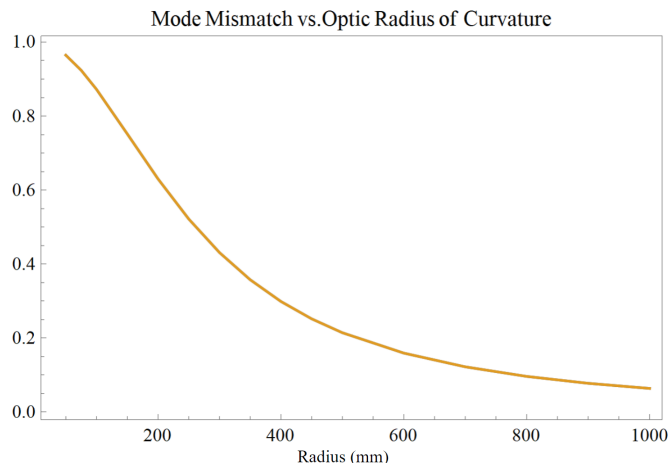


Figure 8: Mode Mismatch as a function of radius of curvature of $Z(R, x, y)$

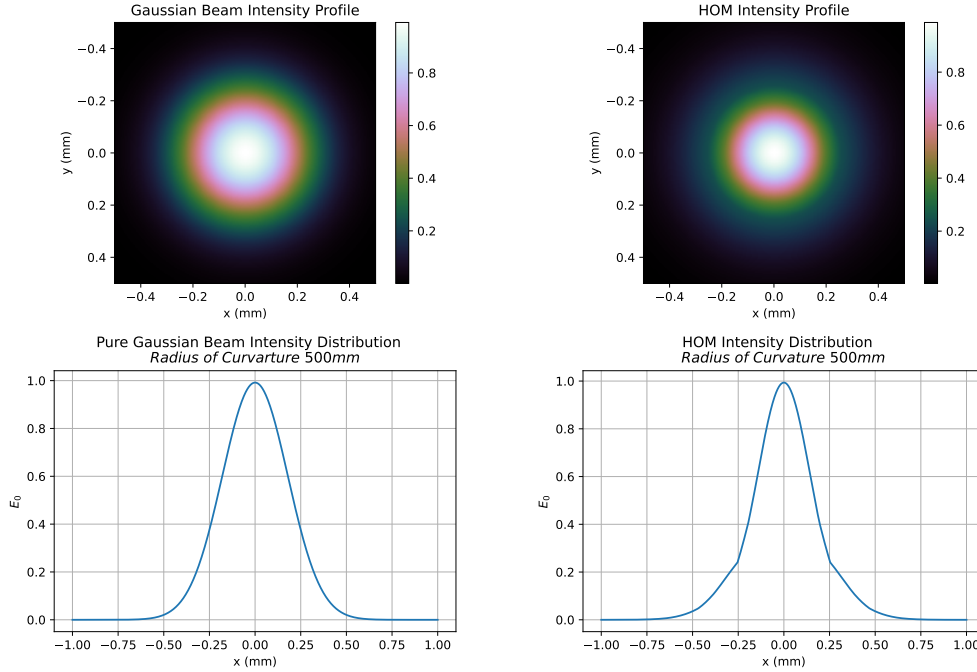


Figure 9: The beam profiles and intensity curves for a pure Gaussian beam compared to a LG modal coupling model evaluated in Python

$Z(R, x, y)$. For ABCD matrix approach, $f = 2R$, so it is evaluated for a lens with 1000mm focal length.

11 Future Steps

11.1 Using Different functions for $Z(R, x, y)$

There is impetus for evaluating a model that propagates through different surfaces of optics. Since lens aberrations arise from the light near the edges of the optic refracting more than the light towards the center, changing the function of curvature may create solutions to the problem [2]. As a result, the next surface to evaluate in the integration is a parabolic surface.

As mentioned in section 8, Mathematica only evaluates for a Taylor approximation made to the sphere

$$Z(R, x, y) = \left(1 - \frac{x^2 + y^2}{R^2}\right)^{1/2}$$

. As a result, it evaluates a second order approximation given in equation 12 that is virtually parabolic. However, this generates the exact same higher order mode distribution, and coupling coefficient plot as a sphere does in Python. Since mathematica does not evaluate either an infinite or finite surface integral of a sphere, the next option is to attempt to construct a Taylor approximation to the evaluation in Python, and evaluate to infinity.

Problems may arise with this. As the code stands now, numerically evaluating the spherical

integration with bounds of -1 to 1 takes about 15 - 30 seconds to complete for each coupling coefficient for a given radius of curvature. Given that the integration takes a large number of steps to evaluate the `dblquad` function, it was shown in Python that the larger the bounds, generally, the longer the integration takes. Looping over an array of values to generate a coupling coefficient vs. R plot takes much longer. It may not be efficient to evaluate to infinity even with a Z surface function as a parabola.

Nonetheless, the next steps would be to define the function

$$Z(R, x, y) = R \left(1 - \frac{x^2 + y^2}{2R^2} \right)$$

as the function to go in the exponential of the integration. Then, different bounds would be tested to see what values to obtain. If the bounds of integration yield a numerical result that is ≤ 1 , encompass the entire beam diameter, and does not take very long to integrate, then it may be a suitable solution to generating data for a parabolic surface.

A more advanced solution would be to take this code, and ssh into the LIGO computer clusters so that the integration in general can be run faster.

Intuitively, different surfaces of curvature should produce different plots. It is expected that the coupling coefficients vary as the function of $Z(R, x, y)$ varies. There is likely a debugging issue in the context of either the Python code or the Mathematica code that needs to be addressed. Nonetheless, the general trend that has already been generated in Python for a spherical function aligns well with spherical aberration theory, and shows how coupling coefficients behave with various lens curvatures.

11.2 Using Two Lenses

Aside from creating different functions for curvature, lens aberrations in general are mitigated through the use of multiple optics [2] [12]. In many high precision focusing optical designs, a multitude of lenses are spaced precisely so that an aberration created by the light

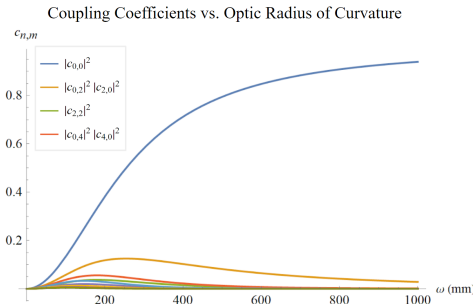


Figure 10: A plot similar to Figure 4 generated in Mathematica, yet $Z(R, x, y)$ is parabolic.

propagating through the first lens can be restored through the second lens.

This may be true for Gaussian optics as well. As higher order modes are created by a lens with a fair amount of curvature, propagation through a second lens may recover those coupled modes back into the pure Gaussian mode.

The first steps to analyzing this start simply. In the Python and Mathematica models, there would be a situation in which a beam at a certain distance z propagates through a convex lens with a fixed front radius of curvature. The most immediate higher order mode is evaluated in the integration, meaning that for HG it would be either the c_{02} or c_{20} mode, and for LG it would be c_{10} . The power of this next higher order mode can be found by taking its absolute value squared. Then, evaluating the propagation at another distance z (representing the distance from the first lens to the second lens), the next higher order mode will act as the beam propagating through the second lens. The integration is then evaluated to determine the coupling of that higher order mode back into the pure Gaussian mode (along with how much it couples into other modes).

Since the integration is normalized, $|c_{nmn'm'}|^2$ for higher order modes back into the Gaussian mode represents the fraction of the power that higher order mode had before propagation through the lens. Therefore, the total fraction of power that gets coupled back into the pure Gaussian mode can be traced back to how much was originally coupled into the higher order mode. This method can then be done for each of the first few higher order modes, and the power that is recoupled back into the pure Gaussian after a second lens propagation can be accurately evaluated.

A concern in this method, is determining if the portion of the beam that is still purely Gaussian after propagating through the first lens, couples into higher order modes after propagation through the second lens more than higher order modes couple back into it. This is a possible challenge when approaching a multi-lens model in the modal coupling method.

However, if this method yields results, and can be debugged so that it becomes applicable to any surface function, there is a vast amount of analysis that can be done. As it stands, higher order modes are a problem in LIGO interferometers, as they create noise in quantum squeezing, and within the optical cavities. Generating a model that can accurately minimize the coupling of higher order modes in its mode matching lenses can greatly improve LIGO's sensitivity.

References

- [1] Yuntao Bai, Gautam Venugopalan, Kevin Kuns, Christopher Wipf, Aaron Markowitz, Andrew R. Wade, Yanbei Chen, Rana X Adhikari, *A phase-sensitive optomechanical amplifier for quantum noise reduction in laser interferometers*. Physical Review. LSC, 2020.
- [2] Jacob Hawthorne, *All You Need to Know About Lens Aberrations in Photography* Schmidt Fine Art Gallery. April 11, 2022. <https://schmidtfineartgallery.com/blogs/news/all-you-need-to-know-about-lens-aberrations-in-photography>
- [3] Andreas Friese, *Finesse 2.0 Manual* GWOptics. <http://www.gwoptics.org/finesse/download/manual.pdf>
- [4] Jenkins A Francis, White E. Harvey, *Fundamentals of Optics* McGraw-Hill Inc. 1957.
- [5] Kenneth Strain, Andreas Freise, Charlotte Bond, Daniel Brown, *Interferometer Techniques for Gravitational-Wave Detection* Chapters 9-11. Physical Review (2015) <https://link.springer.com/content/pdf/10.1007/s41114-016-0002-8.pdf>
- [6] Grant R Fowles, *Introduction to Modern Optics. 2nd Ed.* Dover Publications. 1975.
- [7] H. Kogelnik, T Li., *Laser Beams and Resonators* Applied Optics, 1966.
- [8] Hiro Yamamoto, *LIGO I mirror scattering loss by non smooth surface structure* LSC. July 26, 2007. <http://labcit.ligo.caltech.edu/~hiro/docs/T070170-00.pdf>
- [9] J.M. Burch, A. Gerrard, *Matrix Methods in Optics* Dover Publications, 1974
- [10] Dr. Rana X. Adhikari, Private Consultation
- [11] Shruti Jose Maliakal, Private Consultation
- [12] *Spherical Aberrations* Wikipedia.
- [13] Wolfram Language Documentation. <https://reference.wolfram.com/language/>